



**Manchester
Metropolitan
University**

Higginbottom, Thomas P and Collar, Nigel J and Symeonakis, Elias and Marsden, Stuart J (2019) Deforestation dynamics in an endemic-rich mountain system: Conservation successes and challenges in West Java 1990–2015. *Biological Conservation*, 229. pp. 152-159. ISSN 0006-3207

Downloaded from: <http://e-space.mmu.ac.uk/621954/>

Version: Accepted Version

Publisher: Elsevier

DOI: <https://doi.org/10.1016/j.biocon.2018.11.017>

Usage rights: Creative Commons: Attribution-Noncommercial-No Derivative Works 4.0

Please cite the published version

<https://e-space.mmu.ac.uk>

1 Biological Conservation

2 Volume 229, January 2019, Pages 152-159

3 <https://doi.org/10.1016/j.biocon.2018.11.017>

4
5 *Deforestation dynamics in an endemic-rich*
6 *mountain system: conservation successes and*
7 *challenges in West Java 1990-2015*

8 Thomas P.Higginbottom^{ab}Nigel J.Collar^{ca}EliasSymeonakis^aStuart J.Marsden^a

9
10 School of Science and Environment, Manchester Metropolitan University, Chester Street, a
11 Manchester M1 5GD, UK

12
13 School of Mechanical, Aerospace and Civil Engineering, The University of Manchester, b
14 Sackville Street, M13 9PL, UK

15
16 BirdLife International, David Attenborough Building, Pembroke Street, Cambridge CB2 3QZ, c
17 UK

18 Received 19 May 2018, Revised 22 October 2018, Accepted 14 November 2018, Available online 3
19 December 2018.

20
21 **Abstract**

22 While much has been published on recent rates of forest loss in the Sundaic lowlands, deforestation
23 rates and patterns on Java's endemic-rich mountains have been rather neglected. We used nearly
24 1,000 Landsat images to examine spatio-altitudinal and temporal patterns of forest loss in montane
25 West Java over the last 28 years, and the effectiveness of protected areas in halting deforestation
26 over that period. Around 40% of forest has been lost since 1988, the bulk occurring pre-2000 (2.5%
27 per annum), falling to 1% per annum post-2007. Most deforestation has occurred at lower altitudes
28 (< 1,000 m), both as attrition of the edges of forested mountain blocks as well as the near-total
29 clearance of lower-altitude forested areas. Deforestation within protected areas was rife pre-2000,
30 but greatly decreased thereafter, almost ceasing post-2007 in protected areas of high International
31 Union for Conservation of Nature (IUCN) status. While apparent recent protection against land
32 clearance is welcome, it must be stressed that the area of remaining forest is only 5,234 km², that
33 most accessible lower-altitude forest has already disappeared, and that the extant montane forest is
34 largely fragmented and isolated. The biological value of these forests is huge and without strong

35 intervention we anticipate imminent loss of populations of taxa such as the Javan Slow Loris
36 *Nycticebus javanicus* and Javan Green Magpie *Cissa thalassina*.

37 Keywords: Java, deforestation; protected areas; Landsat, land use/land-cover change

38

39

40

41

42

43

44 Highlights:

- 45 • West Javan mountain forests have endemic biodiversity but a long history of deforestation
- 46 • Since 1990, roughly 40% of forest has been lost, although a decrease in the rate of
47 deforestation has occurred
- 48 • Loss was most prevalent at low altitudes, which were almost completely cleared
- 49 • Forests at higher altitudes and within protected areas fared better
- 50 • Remaining forest is limited to higher altitudes and is vulnerable to fragmentation and
51 clearance

52 1. Introduction

53 Deforestation is one of the main drivers of global biodiversity decline, and a major source of carbon
54 emissions (Houghton et al., 2012; Lawrence and Vandecar, 2015). Information on the extent,
55 severity, and causes of forest loss is therefore critical for a range of disciplines. In recent years,
56 Earth-observation has provided a more accurate and better picture of the global rate and
57 geographical distribution of deforestation (Skole and Tucker 1993; DeFries et al. 2002; Miettinen et
58 al. 2011), highlighting Southeast Asia, and in particular Indonesia, as of major concern (Hansen et al.
59 2013). Within Indonesia, the loss of moist tropical forests on the islands of Borneo and Sumatra,
60 primarily due to the expansion of industrial palm oil plantations, has been well documented (Broich
61 et al., 2011, 2013; Margono et al., 2012; Shevade et al., 2017), but far less attention has been
62 directed towards Java. Indeed, the forests of Java have not received bespoke study and are
63 frequently omitted from published statistics, in part due to the relative sparsity of forest cover
64 remaining since Dutch colonial rule in the eighteenth and nineteenth centuries (Smiet et al. 1990).
65 Such neglect is unfortunate, as these forests possess high levels of biological endemism, with the
66 montane formations on the volcanoes of West Java being particularly rich in unique species
67 (Stattersfield et al., 1998). The West Javan mountains hold all or most of the remaining range of four
68 ‘Critically Endangered’ endemic vertebrates: Javan Slow Loris *Nycticebus javanicus*, Rufous-fronted
69 Laughingthrush *Garrulax rufifrons*, Javan Green Magpie *Cissa thalassina* and Fire Toad *Leptophryne*
70 *cruentata* (IUCN, 2017), and either whole or significant portions of the ranges of many other species
71 of conservation concern (e.g. the ‘Endangered’ Javan Gibbon *Hylobates moloch* and the ‘Vulnerable’
72 Javan Trogon *Apalharpactes reinwardtii* and Javan Cochoa *Cochoa azurea*). These and other
73 endemics are known to be dependent on forest habitats (BirdLife International, 2018).

74 The free availability of large archives of satellite (and notably, since 2008, Landsat) imagery
75 (Wulder et al., 2012; Kennedy et al., 2014) has greatly facilitated the monitoring of land-cover
76 change. These datasets have enabled a shift away from single-image analysis in favour of large-area,
77 automated data-processing chains (Roy et al., 2014), with multiple images amalgamated into target
78 date composites or statistical metric layers (Griffiths et al., 2013). The transition towards multi-
79 image analysis is particularly beneficial in tropical regions where cloud cover is both extensive and
80 frequent, limiting the likelihood of obtaining a cloud-free image (Asner 2001; Hansen et al., 2013).
81 The use of Landsat imagery is preferable for many localities. For example, the use of coarse
82 resolution data from the Moderate-resolution Imaging Spectroradiometer (MODIS) or the Advanced
83 Very High Resolution Radiometer (AVHRR) (e.g. Defries et al., 2002; Hansen et al., 2009) may
84 obscure small-scale patterns which collectively accrue to a large area.

85 In this study, motivated by concern for West Java's endemic biodiversity, we use the Landsat
86 archive to map the deforestation dynamics of the area's remnant upland forests. Our objectives
87 were to: (a) characterise remaining forests; (b) uncover the spatial and temporal occurrence of
88 forest loss events, especially in relation to changes in political order (specifically the termination of
89 the Suharto 'New Order' regime in 1998); and (c) assess the effect of protected areas on the rate of
90 deforestation over recent decades.

91 2. Study area

92 Our study area is ~17,000 km² covering the western uplands of the Indonesian island of Java (Fig 1).
93 We defined uplands as all areas upwards of 400 m above sea level. Analysis was limited to such
94 areas, as these are the location of a majority of remaining upland forest on the island. We focused
95 on 19 West Javan mountains that are of known high biodiversity value (Fig 1b). These mountains
96 include both unprotected areas and protected sites of various International Union for Conservation
97 of Nature (IUCN) designation classes. The climate is broadly tropical, with Köppen climate
98 classifications of Equatorial or Monsoon. Annual temperatures range from 18 to 30°C, with a regular
99 daily average of 28°C. Rainfall is concentrated in the monsoon period November–March, with
100 monthly precipitation around 270 mm. West Javan forests are not dominated by any particular tree
101 species, but common taxa include: Moraceae (*Artocarpus elasticus*), Meliaceae (*Dysoxylum*
102 *caulostachyum* and *Lansium domesticum*), and Lecythidaceae (*Planchonia valida*) (MacKinnon et al.,
103 1993). Java contains twenty volcanoes that have been active in the historical record; accordingly, the
104 regional geology is dominated by relatively recent volcanic rocks, interspersed with marine
105 limestones (Whitten et al., 1996). Java's human population doubled since the 1970s to 145 million
106 today, equating to 1,121 people per km⁻², the highest density in the world (World Bank, 2017). Our
107 study area contains the major cities of Bogor and Bandung, with the Indonesian capital Jakarta just
108 outside the perimeter. A variety of crops are grown within the study area, mainly as smallholdings,
109 with the dominant being rice and coffee (Whitten et al., 1996).

110 3. Methods

111 3.1 Landsat data

112 The Landsat series is the world's longest continuously operating moderate-resolution Earth
113 observation (EO) program. Collecting imagery at 30 m across six spectral bands (plus a thermal
114 band), Landsat is particularly suited for monitoring land-cover change. To map such changes, we
115 produced a series of spectral variability metrics for four epochs corresponding to relevant time

116 periods: 1988–1992, 1998–2000, 2006–2008, and 2014–2016. Spectral metrics are pixel-level
117 statistical summaries calculated from all co-located observations. Metric composites allow the
118 extraction of intra-epochal information on the reflectance of a pixel, and have proved effective for
119 mapping subtle land cover types and improving the accuracy of classifications (Müller et al., 2015).
120 This approach copes more robustly with the problem of persistent cloud cover and atmospheric
121 effects by using all available observations, minimising the contributions of individual pixels which
122 may be compromised, and is therefore well suited to the wet tropics. The composites were
123 generated in Google Earth Engine (Gorelick et al., 2017) from all available Landsat 5 TM and 7 ETM+
124 images. To ensure sufficient observations were present for the calculations, a three-year
125 compositing period was used for the later three epochs, but, owing to lower image availability the
126 1990 composite required a five-year range.

127 All images were processed to surface reflectance using the Landsat Ecosystem Disturbance Adaptive
128 Processing System (LEDAPS), and clouds artefacts masked according to F-mask (Masek et al., 2006;
129 Zhu et al., 2015). For the statistical layers we calculated the mean, standard deviation and a range of
130 percentiles (0, 20, 40, 50, 60, 80, 100%).

131 3.2 Forest change mapping

132 The Landsat spectral variability metrics were classified to produce a land-cover change map. The
133 following classes were mapped: (i) stable forest, (ii) stable non-forest, and loss in the periods (iii)
134 1990–1999, (iv) 1999–2007 and (v) 2007–2015. Training data consisting of 211 polygons were
135 derived from visual bi-temporal comparison of the Landsat composites, in conjunction with high-
136 resolution imagery; forest loss was identified by complete removal of tree cover in the target pixels,
137 whilst stable classes were consistent across all epochs. The classification was undertaken using a
138 Random Forest classifier. Random Forest is a decision-tree-based technique that uses bootstrapped
139 subsets of the training data to generate an ensemble of tree models, which are then aggregated into
140 a final model (Breiman 2001). The internal parameters of the model, the number of trees generated
141 and the number of variable splits, were chosen based on a 10-fold cross validation over a tuning grid
142 of potential values (Kuhn et al., 2017). The classification was developed with the R package
143 randomForest package (version 4.6; Liaw and Wiener, 2002; R Core Team, 2017).

144 To validate our classified map, we first selected a random sample of 75 points per class and
145 calculated the Producer's accuracy. This Producer's accuracy and mapped area per class were used
146 to determine an appropriate stratified sample for a target standard error of 0.5 (Cochran, 1977). The
147 final stratified sample of 539 points was used to calculate Producer's, User's and Overall accuracy

148 scores based on best practice guidelines (Congalton and Green, 2008). Finally, the mapped class
149 areas were adjusted to account for omission errors (Olofsson et al., 2013).

150 3.3 Statistical analysis

151 The roles of altitude, period, and protection status on observed deforestation rates were analysed
152 using a Generalised Linear Mixed Model (GLMM). To generate data for the model, the classified
153 change map was processed as follows. First, the study area was spatially segmented into zones,
154 approximating to mountain catchments. These zones were delineated by assigning each pixel to the
155 most accessible mountain peak, using a cost allocation method with the Shuttle Radar Topography
156 Mission (STRM) Digital Elevation Model (DEM) as a cost surface layer (Longley et al., 2005). This
157 resulted in 28 zones, with an average area of 600 km² ranging from 254 to 1,217 km². Second, each
158 zone was further subdivided according to protection status (protected or unprotected) and altitude,
159 using successive 300 m bands. Finally, the cumulative deforestation rate within each segment for
160 each epoch was then calculated, relative to the starting forest cover in 1990. This resulted in 668
161 unique sample units.

162 A GLMM was built with cumulative deforestation rate as the dependent variable and time
163 period, altitude, and protection status as fixed effects. To account for spatial dependence in the
164 data, mountain zone (catchment area) was added as a random effect. Percentage of forest loss is a
165 proportional response, so a binomial family with logit link function was considered appropriate with
166 the initial number of forest pixels in each segment providing the prior weighting. The R package *lme4*
167 was used for model fitting (Bates et al., 2015), with model R² calculated based on the approach
168 suggested by Nakagawa and Schielzeth (2013) and Johnson (2014). There were insufficient replicates
169 to allow the type of protected area status, according to IUCN, to be included in the model. Therefore
170 the deforestation rates between high protection status (IUCN Classes Ia-II: strict nature reserves and
171 national parks) areas and other sites were compared by corresponding pixel counts.

172 4. Results

173 4.1 Land-cover change classification

174 Our land-cover change classification produced a map (Fig 1 and Fig 2) with an overall accuracy of
175 98% (Table 1). All of the mapped classes had consistently high accuracies, with the least accurate
176 class (loss for 1999–2006) having Producer's and User's accuracies of 0.91 and 0.78 respectively.
177 Adjusting the mapped area estimates using probability-based stratified sampling highlighted a

178 moderate omission of the loss in 1999–2007, with all other classes showing minor biases between
179 the mapped and adjusted areas (Fig 3).

180 4.2 Deforestation rates

181 Over the 1990–2015 period, $3,415 \pm 290$ km² of forest were lost, corresponding to roughly 40% of
182 the initial coverage (Fig 3). By 2015, $5,234 \pm 78$ km² of stable forest remained. Deforestation was
183 greatest in the 1990–1999 period, with $1,923 \pm 24$ km² lost, falling to $1,056 \pm 207$ km² in the period
184 1999–2007 and 436 ± 59 km² for 2007–2015. Deforestation rates equate to 22% (2.5% per annum),
185 16% (2%) and 7% (1%) for the respective periods (Fig 3).

186 Spatially, the greatest concentration of deforestation events was in lower-lying parts of the
187 study area (Fig 1). In particular, forest cover in the relatively low southwestern section was almost
188 completely lost between 1990 and 2007 (Fig 2i). Similar levels of almost total deforestation were
189 identified for the central/southwestern areas (Fig 2ii), where loss continued into the 2007–2015
190 period. The remaining areas of loss were generally located on the edges of contiguous montane
191 forests, with encroachment-style deforestation most apparent (Fig 2iii).

192 4.3 Correlates of deforestation rates

193 The fitted GLMM had good explanatory power with conditional R^2 of 0.45 (full model), with all terms
194 significant at a $p < 0.05$ level (Table 2). The fitted model showed protection status to be a consistent
195 buffer on deforestation, with designated sites exhibiting roughly half the cumulative deforestation of
196 non-designated areas, an effect that was stable across all altitudes (Fig 4). Low-altitude protected
197 sites were subject to non-trivial loss rates (estimated at 10–25% by 2015), yet this contrasts with
198 much greater rates for non-designated areas (30–55%; Fig 4). The majority of forest loss had
199 occurred by 1999 with abatement in deforestation post-2000 most apparent for the 2007–2015
200 period, which exhibited only marginal increases in forest loss, with protected sites showing
201 insignificant changes, particularly at higher altitudes. Sites given high protection status (IUCN Classes
202 Ia-II: strict nature reserves and national parks) enjoyed additional reductions in forest loss,
203 particularly for the 2007–2015 period (Fig 5).

204

205 5. Discussion

206 West Java lost around 40% of its 8,650 km² montane forest in the 25 years since 1990, a figure
207 broadly comparable to other locations in Southeast Asia, e.g. Peninsular Malaysia (Shevade et al.,

208 2017), Kalimantan (Carlson et al., 2012), and Sumatra (Gaveau et al., 2009). What sets it apart from
209 these areas are that (1) the annual rate of forest loss has slowed considerably over time, from a high
210 of 2.2% pre-2000 to 0.5% post-2007, with an important brake being exerted by protected areas,
211 especially strict nature reserves and national parks, and (2) only around 5,500 km² remain of this
212 endemic-rich habitat. Optimism over the decelerating trend in deforestation must be tempered by
213 the extensive loss of forest at altitudes of 300 to 1,800 m, which presumably hold (or held) the most
214 accessible and biodiverse forests. Species that are restricted to or prefer such altitudes are likely to
215 be put under increasing strain across their ranges, especially if deforestation, albeit at slower rates,
216 continues.

217 The post-1999 reduction in forest loss contrasts with reports from wider Indonesia and
218 insular Southeast Asia (Hansen et al., 2013; Kim et al., 2015; Shevade et al., 2017), which show
219 considerable increases in deforestation in the same period. This difference may be attributable to
220 several factors. First, owing to climatic and topographic conditions Java is not well suited to the
221 expansion of industrial tree plantations, particularly palm and rubber, which have driven most post-
222 millennium forest loss in Indonesia and the wider region (Kim et al., 2015). Second, the increased
223 regional autonomy following the democratic transition may have led to a preferential shifting of
224 logging and agriculture to other islands with more lenient planning regulations than Java (Gaveau et
225 al., 2009). Finally, Java was already largely deforested in earlier eras, and the remaining forest is
226 predominantly located at high altitude or on steep slopes, and is therefore less accessible and the
227 associated land less desirable for agriculture (Fig 1, Fig 5). The contrast between Java and wider
228 Indonesia highlights the need for tailored studies addressing localised factors.

229 High rates of deforestation across insular Southeast Asia during the 1990s are well
230 documented (Hansen et al., 2009; Kim et al., 2015), and relate to both political-economic and
231 environmental factors. The 1990s were an economic boom period for Southeast Asia, with
232 increasing commodity prices and favourable exchange rates driving growth in both agricultural and
233 hardwood exports (Mason, 2001). This economic situation combined with lax forest protection laws
234 encouraged widespread logging and agricultural expansion (Hansen et al., 2009). Environmentally,
235 the 1997 El Niño event was severe, leading to widespread forest fires across the region (Page et al.,
236 2002).

237 The last two epochs of our study postdate the Asian financial crisis of July 1997 and the
238 associated economic consequences; within six months inflation peaked at 80%, and gross domestic
239 product dropped by 47% (World Bank 2017). The resignation of President Suharto in May 1998
240 ended the 42-year New Order dictatorship and initiated a shift to representative democracy. This

241 period was also marked by a number of forestry legislation changes, such as a round wood export
242 ban in 2001, aiming to curtail illegal logging (Resosudarmo and Yusuf, 2006). Interestingly, our
243 results contradict those of Miettinen et al. (2011), who observed a 4.2% increase in forest cover on
244 Java between 2000 and 2010. We attribute this to two factors: first, we did not attempt to map
245 reforestation, so did not account for gains; and second, Miettinen et al. (2011) used 250 m MODIS
246 data, compared to the 30 m Landsat imagery used here, so our analysis probably identified smaller
247 clearances missed by the coarser MODIS data.

248 Assessing the efficacy of protected areas is critical for ensuring long-term conservation (e.g.
249 Mallari et al. 2013, 2016). Java's officially protected areas have fared reasonably well over the study
250 period, especially since 2000 compared to those in Sumatra and Borneo, where encroachment
251 through small-scale logging and agriculture is rife (Curran et al., 2004; Gaveau et al., 2009).
252 Furthermore, the high altitude of most parks and reserves has minimised the displacement of
253 logging to unprotected areas (Gaveau et al., 2009). Since 1999, forest loss in highly protected areas
254 (IUCN Classes Ia and II) has been minimal, with a < 0.1% rate since 2007, but further study of the
255 efficacy of different protection levels would be valuable, as our small sample size precluded robust
256 modelling. Moreover, this welcome trend must be set against an extremely high baseline rate in the
257 1990s when forests below 1,000 m suffered a decline rate of 55% overall and 20% inside protected
258 areas. As a consequence, only 2,500 km² of low-altitude forest remains (around 20% coverage). This
259 will have detrimental effects for connectivity between the better-preserved highland forests, with
260 increasing separation of major mountain chains and individual peaks (Fig 2ii-iii). Species movement
261 modelling to identify connectivity corridors between the remaining forest and the bottlenecks to
262 these connections would benefit conservation planning (e.g. Bleyhl et al., 2017). Crucially, forest
263 loss, however slow, continues in montane West Java, not only compromising the future of the
264 island's most distinctive fauna and flora but also inevitably risking ecosystem services such as water
265 retention and regulation. Efforts to enhance the protection status of those montane forests
266 currently with no or low IUCN protected area designation, field surveys to assess the viability of
267 populations of endemic and threatened taxa (many mountains have not been visited by ecologists
268 for decades), and protection, by whatever means, of lower-altitude montane forests, are, therefore,
269 matters of great urgency.

270

271 References

- 272 Asner, G.P., 2001. Cloud cover in Landsat observations of the Brazilian Amazon. *International Journal*
273 *of Remote Sensing*, 22(18), pp.3855-3862.
- 274 Bates, D., Mächler, M., Bolker, B. and Walker, S., 2015. Fitting linear mixed-effects models using
275 lme4. *Journal of Statistical Software*, 67(1) pp1-48.
- 276 BirdLife International 2018, Country profile: Indonesia. Available from
277 <http://www.birdlife.org/datazone/country/indonesia>. Checked: 2018-07-25
- 278 Breiman, L., 2001. Random forests. *Machine learning*, 45(1), pp.5-32.
- 279 Bleyhl, B., Baumann, M., Griffiths, P., Heidelberg, A., Manvelyan, K., Radeloff, V.C., Zazanashvili, N.
280 and Kuemmerle, T., 2017. Assessing landscape connectivity for large mammals in the Caucasus using
281 Landsat 8 seasonal image composites. *Remote Sensing of Environment*, 193, pp.193-203.
- 282 Broich, M., Hansen, M., Stolle, F., Potapov, P., Margono, B.A. and Adusei, B., 2011. Remotely sensed
283 forest cover loss shows high spatial and temporal variation across Sumatera and Kalimantan,
284 Indonesia 2000–2008. *Environmental Research Letters*, 6(1), p.014010.
- 285 Broich, M., Hansen, M., Potapov, P. and Wimberly, M., 2013. Patterns of tree-cover loss along the
286 Indonesia–Malaysia border on Borneo. *International Journal of Remote Sensing*, 34(16), pp.5748-
287 5760.
- 288 Carlson, K.M., Curran, L.M., Ratnasari, D., Pittman, A.M., Soares-Filho, B.S., Asner, G.P., Trigg, S.N.,
289 Gaveau, D.A., Lawrence, D. and Rodrigues, H.O., 2012. Committed carbon emissions, deforestation,
290 and community land conversion from oil palm plantation expansion in West Kalimantan, Indonesia.
291 *Proceedings of the National Academy of Sciences*, 109(19), pp.7559-7564.
- 292 Cochran W.G, 1977. Sampling techniques. Wiley, New York.
- 293 Congalton, Russell G., and Green K. 2008. Assessing the accuracy of remotely sensed data: principles
294 and practices. CRC press, Boca Raton.
- 295 Curran, L.M., Trigg, S.N., McDonald, A.K., Astiani, D., Hardiono, Y.M., Siregar, P., Caniago, I. and
296 Kasischke, E., 2004. Lowland forest loss in protected areas of Indonesian Borneo. *Science*, 303(5660):
297 1000-1003.

298 DeFries, R.S., Houghton, R.A., Hansen, M.C., Field, C.B., Skole, D. and Townshend, J., 2002. Carbon
 299 emissions from tropical deforestation and regrowth based on satellite observations for the 1980s
 300 and 1990s. *Proceedings of the National Academy of Sciences*, 99(22), 14256-14261.

301 Eaton, J.A., Shepherd, C.R., Rheindt, F.E., Harris, J.B.C., van Balen, S.B., Wilcove, D.S. & Collar, N.J.
 302 2015. Trade-driven extinctions and near-extinctions of avian taxa in Sundaic Indonesia. *Forktail* 31:
 303 1-12.

304 Gaveau, D.L., Epting, J., Lyne, O., Linkie, M., Kumara, I., Kanninen, M. and Leader-Williams, N., 2009.
 305 Evaluating whether protected areas reduce tropical deforestation in Sumatra. *Journal of*
 306 *Biogeography*, 36(11), 2165-2175.

307 Gorelick, N., Hancher, M., Dixon, M., Ilyushchenko, S., Thau, D. and Moore, R., 2017. Google Earth
 308 Engine: Planetary-scale geospatial analysis for everyone. *Remote Sensing of Environment* 202 pp. 18-
 309 27

310 Griffiths, P., S. Van Der Linden, T. Kuemmerle, and P. Hostert ., 2013. A pixel-based Landsat
 311 compositing algorithm for large area land cover mapping. *IEEE Journal of Selected Topics in Applied*
 312 *Earth Observations and Remote Sensing*, 6.(5), 2088 2101

313 Hansen, M.C., Potapov, P.V., Moore, R., Hancher, M., Turubanova, S.A., Tyukavina, A., Thau, D.,
 314 Stehman, S.V., Goetz, S.J., Loveland, T.R. and Kommareddy, A., 2013. High-resolution global maps of
 315 21st-century forest cover change. *Science*, 342(6160), pp.850-853.

316 Hansen, M.C., Stehman, S.V., Potapov, P.V., Arunarwati, B., Stolle, F. and Pittman, K., 2009.
 317 Quantifying changes in the rates of forest clearing in Indonesia from 1990 to 2005 using remotely
 318 sensed data sets. *Environmental Research Letters*, 4(3), p.034001.

319 Houghton, R.A., House, J.I., Pongratz, J., Van Der Werf, G.R., DeFries, R.S., Hansen, M.C., Quéré, C.L.
 320 and Ramankutty, N., 2012. Carbon emissions from land use and land-cover change. *Biogeosciences*,
 321 9(12), pp.5125-5142.

322 IUCN 2017. The IUCN Red List of Threatened Species. Version 2017-3. <<http://www.iucnredlist.org>>.

323 Johnson, P.C., 2014. Extension of Nakagawa & Schielzeth's R^2 GLMM to random slopes models.
 324 *Methods in Ecology and Evolution*, 5(9), pp.944-946.

325 Kennedy, R.E., Andréfouët, S., Cohen, W.B., Gómez, C., Griffiths, P., Hais, M., Healey, S.P., Helmer,
 326 E.H., Hostert, P., Lyons, M.B. and Meigs, G.W., 2014. Bringing an ecological view of change to
 327 Landsat-based remote sensing. *Frontiers in Ecology and the Environment*, 12(6), pp.339-346.

328 Kim, D.H., Sexton, J.O. and Townshend, J.R., 2015. Accelerated deforestation in the humid tropics
329 from the 1990s to the 2000s. *Geophysical Research Letters*, 42(9), pp.3495-3501.

330 Lawrence, D. and Vandecar, K., 2015. Effects of tropical deforestation on climate and agriculture.
331 *Nature Climate Change*, 5(1), pp.27-36.

332 Liaw, A. and Wiener, M., 2002. Classification and regression by randomForest. *R news*, 2(3), pp.18-
333 22.

334 Longley, P.A., Goodchild, M.F., Maguire, D.J. and Rhind, D.W., 2005. Geographic information systems
335 and science. John Wiley & Sons.

336 Mason, A., 2001. Population change and economic development in East Asia: Challenges met,
337 opportunities seized. Stanford University Press.

338 Mallari, N. A. D., Collar, N. J., McGowan, P. J. K. & Marsden, S. J. (2013) Science-driven management
339 of protected areas: a Philippine case study. *Env. Mgmt.* 51: 1236-1246.

340 Mallari, N. A. D., Collar, N. J., McGowan, P. J. K. & Marsden, S. J. (2016) Philippine protected areas
341 are not meeting the biodiversity coverage and management effectiveness requirements of Aichi
342 Target 11. *Ambio* 45: 313-322.

343 Masek, J.G., Vermote, E.F., Saleous, N.E., Wolfe, R., Hall, F.G., Huemmrich, K.F., Gao, F., Kutler, J. and
344 Lim, T.K., 2006. A Landsat surface reflectance dataset for North America, 1990-2000. *IEEE Geoscience
345 and Remote Sensing Letters*, 3(1), pp.68-72.

346 Margono, B.A., Turubanova, S., Zhuravleva, I., Potapov, P., Tyukavina, A., Baccini, A., Goetz, S. and
347 Hansen, M.C., 2012. Mapping and monitoring deforestation and forest degradation in Sumatra
348 (Indonesia) using Landsat time series data sets from 1990 to 2010. *Environmental Research
349 Letters*, 7(3), p.034010.

350 MacKinnon, J.R. and Phillipps, K., 1993. A field guide to the birds of Borneo, Sumatra, Java, and
351 Bali—the Greater Sunda Islands. Oxford University Press.

352 Miettinen, J., Shi, C. and Liew, S.C., 2011. Deforestation rates in insular Southeast Asia between 2000
353 and 2010. *Global Change Biology*, 17(7), pp.2261-2270.

354 Müller, H., Rufin, P., Griffiths, P., Siqueira, A.J.B. and Hostert, P., 2015. Mining dense Landsat time
355 series for separating cropland and pasture in a heterogeneous Brazilian savanna landscape. *Remote
356 Sensing of Environment*, 156, pp.490-499.

357 Nakagawa, S. and Schielzeth, H., 2013. A general and simple method for obtaining R² from
358 generalized linear mixed-effects models. *Methods in Ecology and Evolution*, 4(2), pp.133-142.

359 Olofsson, P., Foody, G.M., Stehman, S.V. and Woodcock, C.E., 2013. Making better use of accuracy
360 data in land change studies: Estimating accuracy and area and quantifying uncertainty using
361 stratified estimation. *Remote Sensing of Environment*, 129, pp.122-131.

362 Page, S.E., Siegert, F., Rieley, J.O., Boehm, H.D.V., Jaya, A. and Limin, S., 2002. The amount of carbon
363 released from peat and forest fires in Indonesia during 1997. *Nature*, 420(6911), pp.61-65.

364 R Core Team, 2017. R: A Language and Environment for Statistical Computing. R Foundation for
365 Statistical Computing. <https://www.R-project.org>

366 Resosudarmo, B.P. and Yusuf, A.A., 2006. Is the log export ban an efficient instrument for economic
367 development and environmental protection? The case of Indonesia. *Asian Economic Papers*, 5(2),
368 pp.75-104.

369 Roy, D.P., Wulder, M.A., Loveland, T.R., Woodcock, C.E., Allen, R.G., Anderson, M.C., Helder, D.,
370 Irons, J.R., Johnson, D.M., Kennedy, R. and Scambos, T.A., 2014. Landsat-8: Science and product
371 vision for terrestrial global change research. *Remote sensing of Environment*, 145, pp.154-172.

372 Shevade, V.S., Potapov, P.V., Harris, N.L. and Loboda, T.V., 2017. Expansion of industrial plantations
373 continues to threaten Malayan tiger habitat. *Remote Sensing*, 9(7), p.747

374 Skole, D. and Tucker, C., 1993. Evidence for tropical deforestation, fragmented habitat, and
375 adversely affected habitat in the Brazilian Amazon: 1978–1988. *Science*, 260(5116), pp.1905-1910.

376 Smiet, A.C., 1990. Forest ecology on Java: conversion and usage in a historical perspective. *Journal of*
377 *Tropical Forest Science*, pp.286-302

378 Stattersfield, A. J., Crosby, M. J., Long, A. J. and Wege, D. C. 1998. Endemic bird areas of the world:
379 priorities for biodiversity conservation. Cambridge, U.K.: BirdLife International (Conservation Series
380 7).

381 World Bank. (2017). Indonesia Data Profile. Available:
382 <https://data.worldbank.org/country/indonesia>. Last accessed December 2017.

383 Whitten, T., Soeriatmadja, R.E. and Afiff, S.A., 1996. Ecology of Java & Bali (Vol. 2). Oxford
384 University Press.

385 Wulder, M.A., Masek, J.G., Cohen, W.B., Loveland, T.R. and Woodcock, C.E., 2012. Opening the
386 archive: How free data has enabled the science and monitoring promise of Landsat. *Remote Sensing*
387 *of Environment*, 122, pp.2-10.

388 Zhu, Z., Wang, S. and Woodcock, C.E., 2015. Improvement and expansion of the Fmask algorithm:
389 cloud, cloud shadow, and snow detection for Landsats 4–7, 8, and Sentinel 2 images. *Remote Sensing*
390 *of Environment*, 159, pp.269-277.

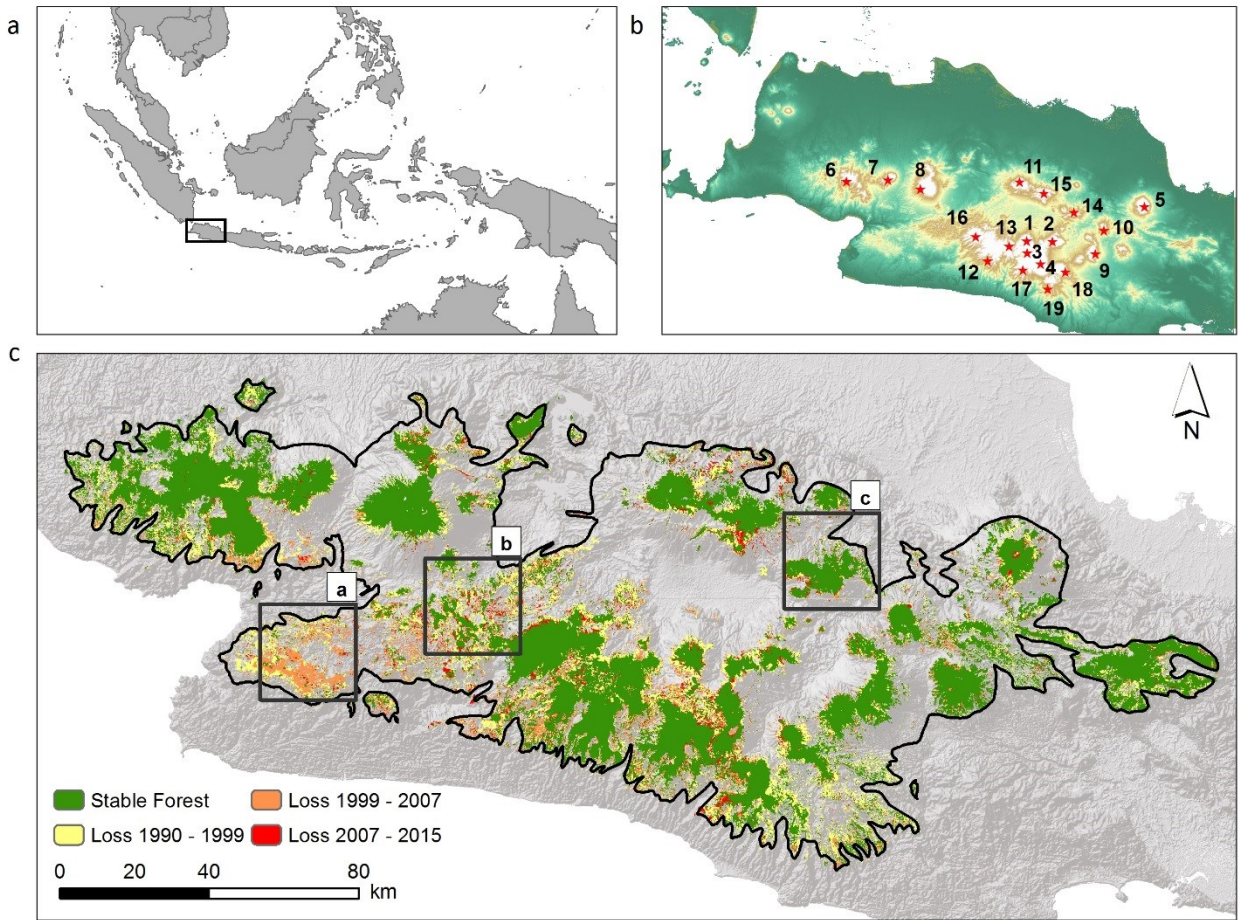
391

392

393

394

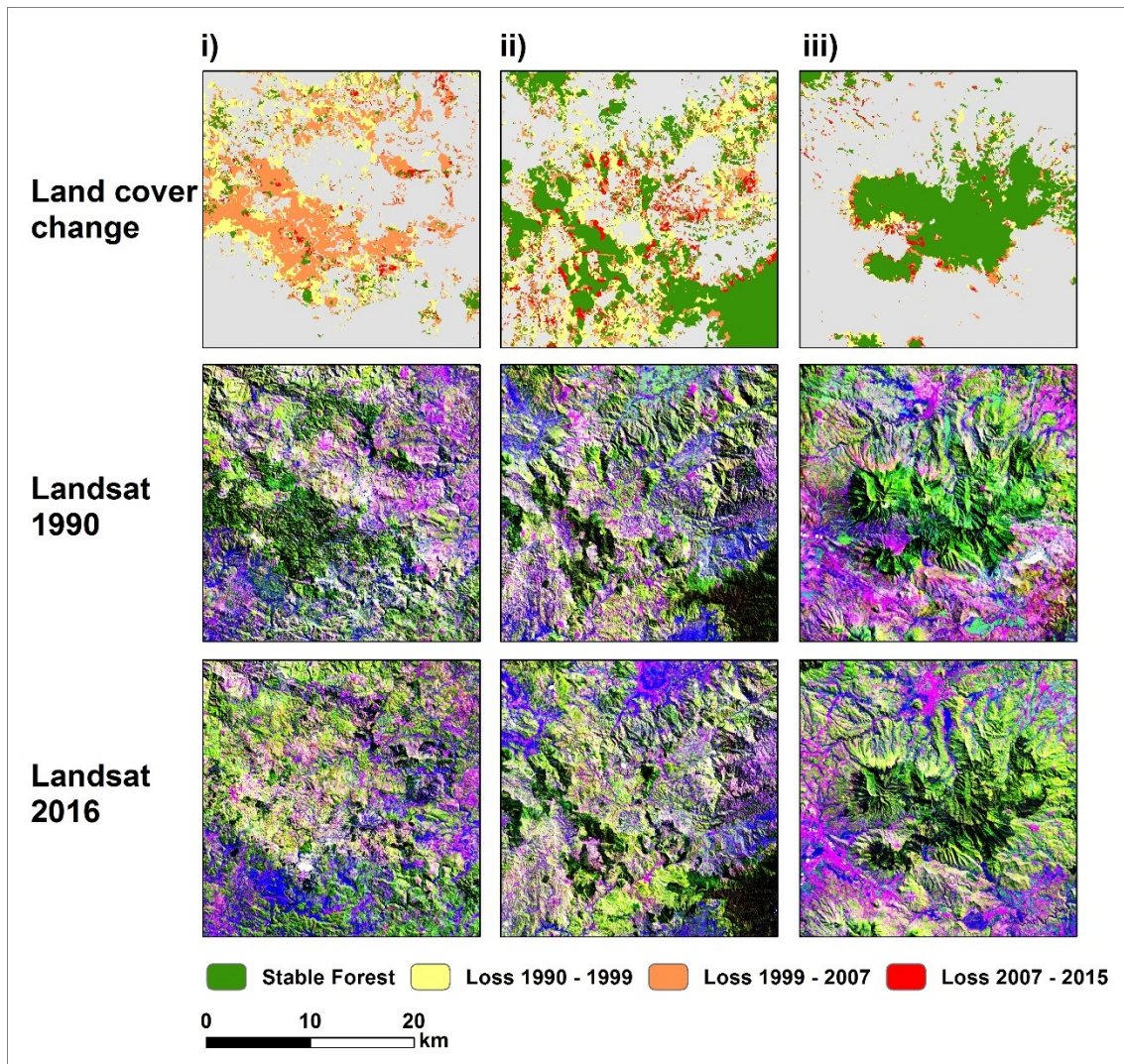
395



397

398 **Fig 1** (a) Location of the study area within Southeast Asia; (b) Digital Elevation Model (DEM) of the
 399 study location with stars indicating the mountain sites selected for further study; (c) land-cover
 400 change map with the 400 m contour highlighted in black (grey boxes refer to the subset images in
 401 Fig 2)

402

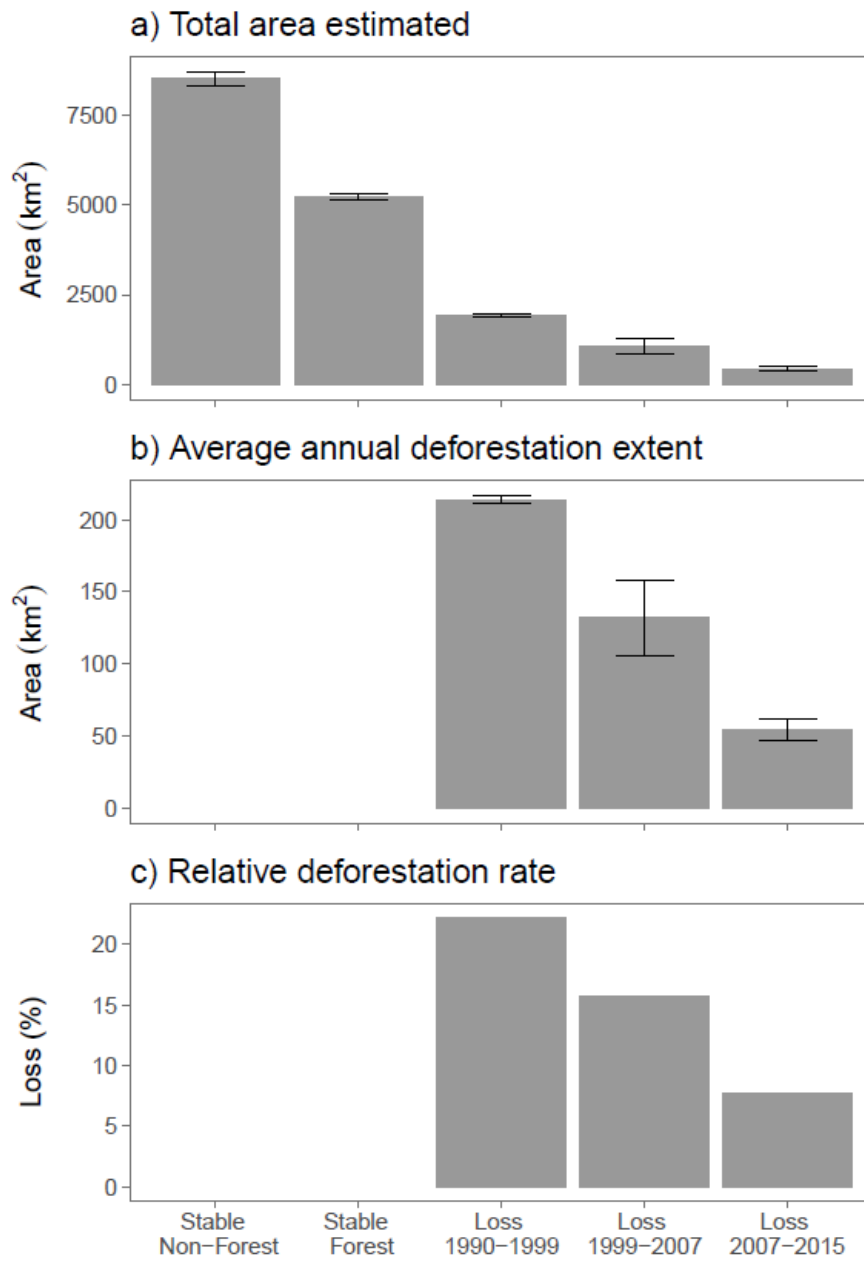


403

404 **Fig 2** Results of the land-cover change classification (top row), 1990 Landsat 5 median composite
 405 (middle row), and 2016 Landsat 8 median composite (bottom row), for the three areas shown in Fig
 406 1. Band association in the Landsat RGB false colour composites: R = shortwave infrared; G = near
 407 infrared; B = red

408

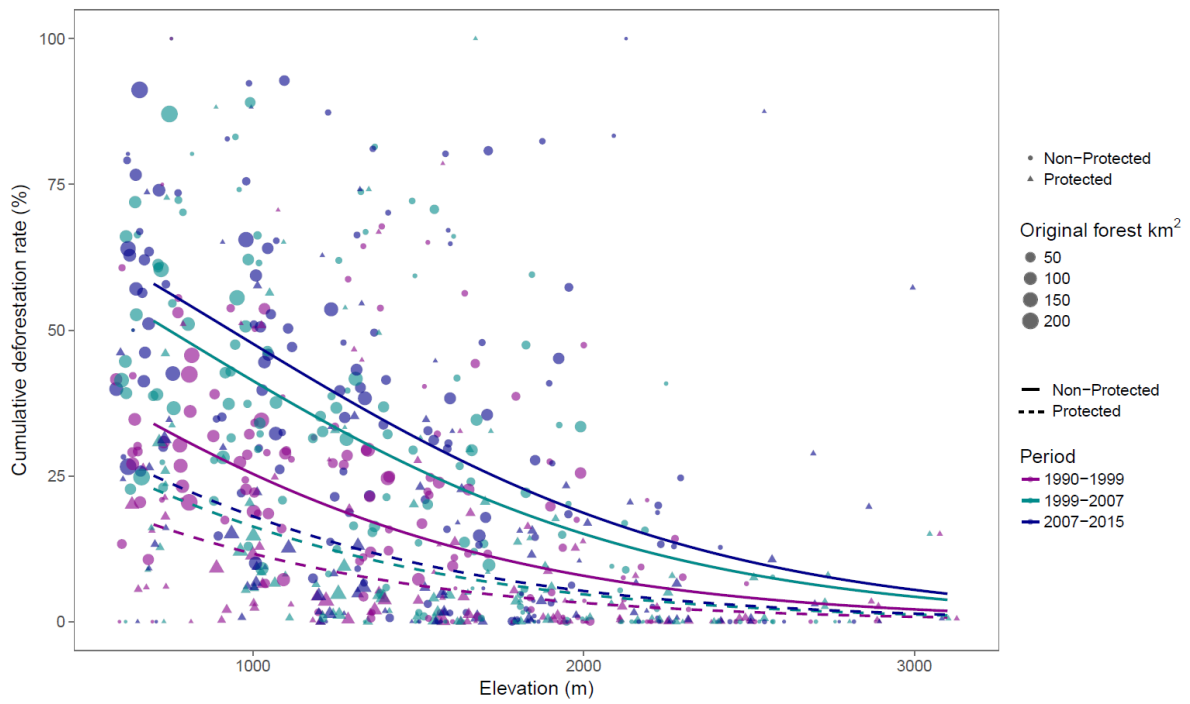
409



410

411 **Fig 3** Area-adjusted estimated, with 95% confidence intervals, for the land-cover change classes
 412 covering the whole study area

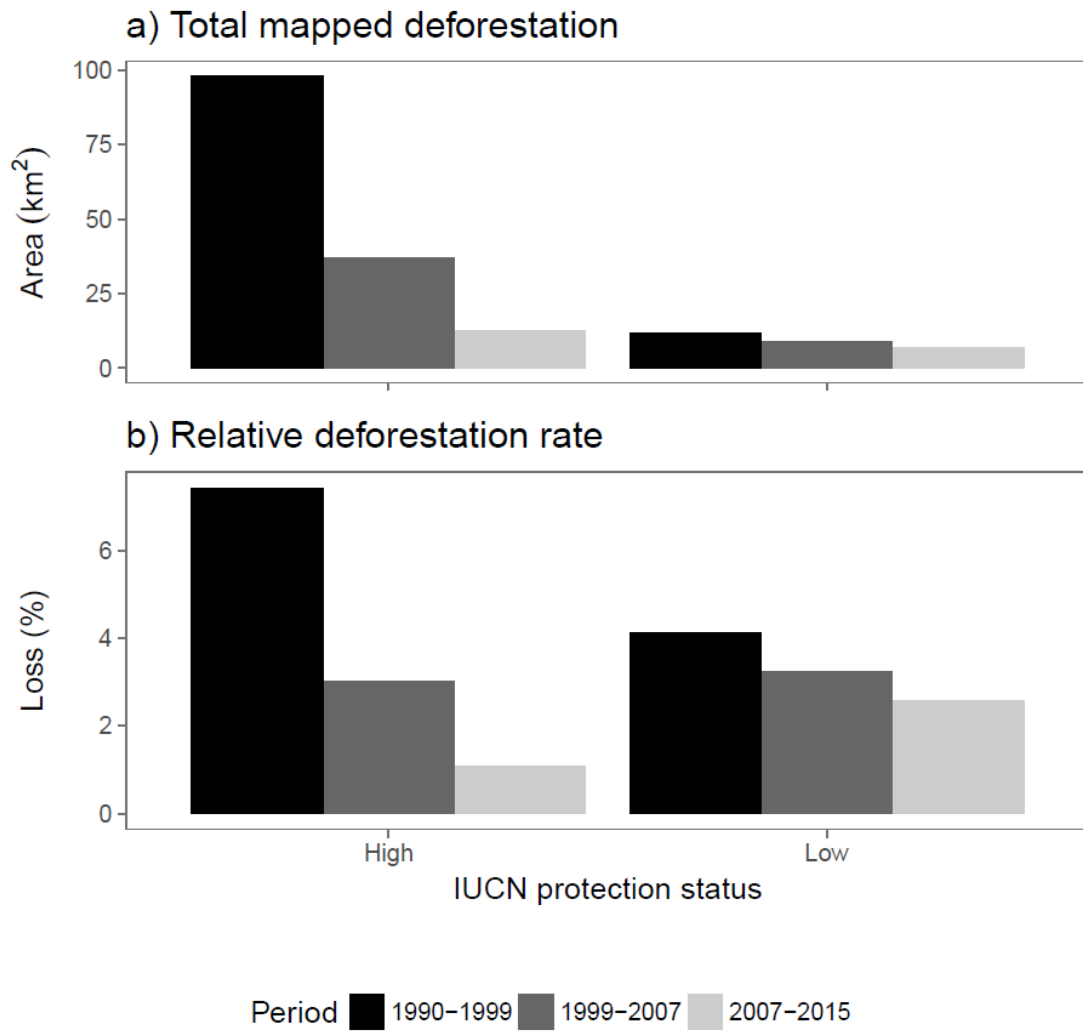
413



414

415 **Fig 4** Role of altitude, protection, and period on cumulative deforestation rate. Curves are derived

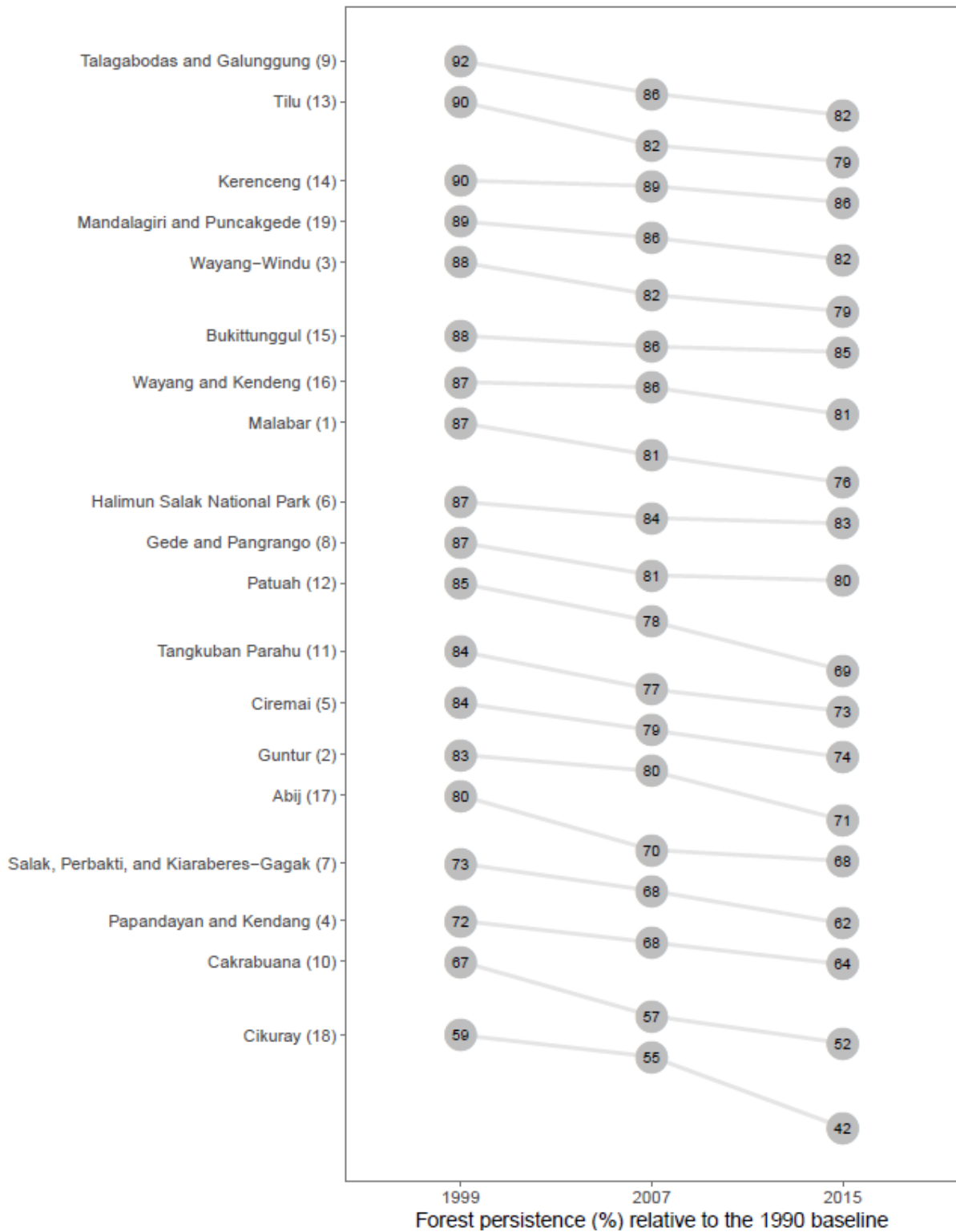
416 from a binomial Generalised Linear Mixed Model (GLMM).



417

418 **Fig 5** Total mapped deforestation per International Union for Conservation of Nature (IUCN)
 419 protected area status

420



421

422 **Fig 6** Forest persistence, as a percent of the 1990 baseline across the three epochs for each
 423 mountain site. Numbers next to names relate to the mountains in Figure 1

424

425

426

427

428

429

430 Tables

432 Table 1 Error matrix and derived accuracy for the land-cover change map

		REFERENCE					Total
		<i>Stable forest</i>	<i>Stable non-forest</i>	<i>Loss 1990–1999</i>	<i>Loss 1999–2007</i>	<i>Loss 2007–2015</i>	
MAPPED	<i>Stable forest</i>	131	0	0	1	0	132
	<i>Stable non-forest</i>	0	183	0	4	0	187
	<i>Loss 1990–1999</i>	0	0	74	0	0	74
	<i>Loss 1999–2007</i>	0	0	1	69	6	76
	<i>Loss 2007–2015</i>	0	0	0	1	69	70
	<i>Total</i>	131	183	75	75	75	539
	User's	0.99	0.98	1	0.91	0.99	
	Producer's	1	1	0.99	0.78	0.84	
	<i>Overall</i>	0.98					

433

434

435

436

437

438

439

440

441

442

443

444 Table 2 Odds ratio effects and 95% confidence intervals (CI) for the fixed and random components of
 445 the Generalised Linear Mixed Model (GLMM). The model resulted in a marginal R² of 0.3 (only fixed
 446 effects) and conditional R² of 0.45 (full model).

	Response		
	<i>Odds ratio</i>	<i>CI</i>	<i>p</i>
Intercept	0.17	0.13–0.24	<0.001
Altitude	0.45	0.45–0.45	<0.001
<i>Period 1999–2007</i>	2.07	2.06–2.08	<0.001
<i>Period 2007–2015</i>	2.68	2.67–2.70	<0.001
Status *Protected	0.39	0.38–0.40	<0.001
Period 1999–2007: Status Protected	0.71	0.70–0.73	<0.001
Period 2007–2015: Status Protected	0.62	0.61–0.64	<0.001
τ _{00, Zone}		0.624	
N _{zone}		27	
ICC _{zone}		0.159	
Observations		668	

447

448